Korean Chem. Eng. Res., 64(3), 105171 (2026)
https://doi.org/10.9713/kcer.2026.64.3.105171
PISSN 0304-128X, EISSN 2233-9558

The Design Of Continuous Fixed Bed Reactor For Biofuel Production Over Fischer-tropsch Synthesis

Jimmy*,†, Endah Kusuma Rastini, Aman Santoso*** and Elvianto Dwi Daryono***

*Department of Chemical Engineering, National Institute of Technology (ITN)Malang
Jln. Bendungan Sigura-gura No. 2 Malang, East Java, Indonesia, 65145
**Department of Mechanical Engineering, National Institute of Technology (ITN)Malang
Jln. Bendungan Sigura-gura No. 2 Malang, East Java, Indonesia, 65145
***Department of Chemistry, Malang State University
Jln. Semarang No. 5 Malang, East Java, Indonesia, 65145
(Received 28 December 2024; Received in revised from 5 March 2025; Accepted 7 May 2026)

Abstract – The development of continuous fixed-bed reactors is essential for studying reaction behavior and catalyst performance under elevated temperature and pressure. However, many Fischer–Tropsch (FT) reactor designs lack detailed specifications, leading to challenges in stability and reproducibility. This study presents a continuous fixed-bed tubular reactor for FT synthesis using synthesis gas (CO and H_2) with controlled temperature, pressure, and flow rate. The reactor employed a ceramic heater with PID controller and a modified double-stage regulator, achieving stable operation at 20 bar (±0.2 bar) and temperature fluctuations within ±3–4°C after reaching steady state over extended continuous operation periods up to 96 hours. The reaction produced two liquid phases: hydrocarbon-rich products in the upper layer and oxygenated compounds in the lower layer. GC-MS peak area analysis showed hydrocarbons were dominated by alkanes (C7–C25), with kerosene as the main fraction. Increasing catalyst weight raised alkane selectivity (up to 99.96%) and straight-chain hydrocarbons (up to 72.03%). This trend was attributed to reduced gas hourly space velocity (GHSV) and increased residence time, which promoted hydrogenation and chain growth. These results demonstrated stable reactor performance, with product distribution reported as relative composition rather than absolute yield.

Key words: Fischer-tropsch, Fixed-bed reactor, Gas hourly space velocity (GHSV), Design, Pressure control, Temperature control

1. Introduction

In the chemical industry, many heterogeneous reactions, such as hydrogenation, reforming, dehydrogenation, and polymerization, are carried out under high-temperature and high-pressure conditions [1–3]. Laboratory-scale fixed-bed reactors play an important role in chemical engineering research, particularly for studying reaction behavior, catalyst development, and process evaluation under controlled conditions [4]. The stability of operating parameters in such systems is critical, requiring precise control of temperature, pressure, and reactant flow to ensure reliable and reproducible results. Therefore, the implementation of automatic control systems, such as proportional–integral–derivative (PID) controllers and high-accuracy sensors, is essential to maintain steady-state operation and minimize fluctuations that may affect reaction performance [5,6].

1-1. Reactor designs for fischer-tropsch synthesis

Fischer–Tropsch (FT) synthesis is a process that converts synthesis gas (CO and H_2) into liquid hydrocarbons through catalytic reactions, providing a potential route for biofuel production [7]. The process generally involves the formation of long-chain hydrocarbons (wax) via polymerization reactions, followed by secondary reactions such as cracking and hydrogenation that produce shorter hydrocarbons in the range of C_5–C_{19}, corresponding to gasoline, kerosene, and diesel fractions [8]. Various reactor configurations have been investigated for FT synthesis, including batch reactors, slurry-phase reactors, and fixed-bed reactors. Among these, continuous fixed-bed reactors are widely used due to their relatively simple design, ease of operation, and capability to operate under high-pressure condition [9]. In addition, they offer advantages in terms of scalability and process control. However, many previous studies have not provided detailed design specifications, particularly regarding control systems and operational stability, which are critical for ensuring reproducible and reliable performance [10].

1-2. Control systems for fixed-bed reactors

Proper temperature regulation is crucial to prevent catalyst deactivation as a result of sintering and contamination, as Fischer-Tropsch synthesis is highly exothermic [11]. Reactor design parameters, such as bed length and tube diameter, also influence heat and mass transfer, where smaller diameters and elongated beds can enhance

† To whom correspondence should be addressed.
E-mail: j_roring@yahoo.com

heat dissipation and improve temperature control [12]. In addition to reactor geometry, control systems play a key role in maintaining stable operating conditions. The integration of proportional–integral–derivative (PID) controllers, mass flow meters, and pressure regulators enables precise control of temperature, pressure, and reactant flow, ensuring that the reaction proceeds within the desired operating window [13]. Previous studies have shown that improved control strategies, including precise flow monitoring and multi-zone temperature regulation, can significantly enhance reactor performance and product selectivity [14]. However, comprehensive evaluations of integrated control systems, particularly in relation to long-term operational stability, remained limited in the current literature [15].

1-3. Catalysts and their role in fischer-tropsch reactions

The performance of Fischer–Tropsch reactors is strongly influenced by catalyst type and composition [4]. Metal-based catalysts such as cobalt (Co), iron (Fe), nickel (Ni), and ruthenium (Ru) are commonly used to facilitate CO hydrogenation and hydrocarbon chain growth, while acidic catalysts such as HZSM-5 are often incorporated to promote secondary reactions, including hydrocracking and isomerization, which influence product distribution [16]. The selection of operating temperature is closely related to catalyst type. Low-temperature FTS (200–240°C), typically using Co-based catalysts, favours the formation of long-chain hydrocarbons and waxes, whereas high-temperature FTS (300–350°C), commonly associated with Fe-based catalysts, promotes the formation of gasoline-range hydrocarbons and light olefins [17]. Recent developments in catalyst design, including bimetallic systems and structured supports, have been explored to enhance hydrocarbon distribution and catalyst performance [18]. However, challenges related to catalyst stability, such as sintering, carbon deposition, and deactivation, remained significant issues in Fischer–Tropsch research [19].

1-4. Research gap and objectives

Although significant progress has been made in reactor development for Fischer–Tropsch synthesis, many previous studies lack detailed descriptions of reactor components, control systems, and catalyst configuration, which are essential for ensuring stable and reproducible operation [10]. Furthermore, the influence of operational factors such as gas hourly space velocity (GHSV) and residence time is not always explicitly considered in relation to reactor configuration, despite their important role in determining product distribution [6]. To address these gaps, this study aims to design and evaluate a continuous fixed-bed tubular reactor for Fischer–Tropsch synthesis with integrated control of temperature, pressure, and flow rate. A modified pressure control system and automated monitoring are implemented to ensure stable operation under laboratory-scale conditions. The reactor performance is assessed in terms of operational stability and hydrocarbon product distribution based on GC-MS analysis.

1-5. Novelty and advantages of this reactor design

This study presents a continuous fixed-bed reactor design with an integrated control system aimed at improving operational stability under laboratory-scale conditions. Compared to previously reported systems, the proposed design incorporates a modified pressure control approach, precise temperature regulation, and an optimized catalyst configuration to maintain stable operating conditions. The integration of pressure, temperature, and flow control systems contributes to consistent reactor performance with reduced fluctuations during operation. In addition, the use of hot and cold traps and improved thermal management helps to mitigate issues such as temperature overshoot and potential hotspot formation, which are common challenges in Fischer–Tropsch reactors [7]. This work provides detailed design specifications for reactor components and control systems, addressing the limited reporting in previous studies [20]. The proposed configuration offers a practical and cost-effective approach for laboratory-scale FTS applications and provides a foundation for further development toward larger-scale reactor systems.

2. Methods

This study will discuss the design of a Fischer-Tropsch reactor, the stability of operating conditions, and the overall performance of the reactor. The reactor was designed to meet the needs of a continuous process that must maintain a balance between temperature, pressure, feed gas flow rate, and product flow rate. The selection of equipment specifications was adjusted to the operating conditions to be used. Catalogs of each component served as guidelines for making appropriate selections. Temperature control utilized an electric heater capable of heating up to 400°C, supported by a temperature controller, thermocouple, relay, and contactor. Heat insulation was also required to reduce heat loss, ensuring energy efficiency. Pressure control in the reactor, set at 20 bar, and at the reactor outlet, set at 1 bar, required specific controllers that were cost-effective. The feed gas flow rate of 25 mL/min was controlled by using a specialized valve that can be calibrated to deliver gas according to the needs.

The stability of reaction conditions was tested by collecting data on pressure, temperature, and flow rate at 2-minute intervals during the first 1 hours, followed by hourly observations for the next 7 hours. Data from the initial process was used to analyze the time required to reach steady-state conditions.

The performance of the continuous fixed bed reactor was assessed using Fischer-Tropsch Synthesis with a 10Fe-90Co/meso-HZSM-5 catalyst at 250°C and 20 bar pressure. The synthesis gas flow rate was 25 mL/min (30% CO, 60% H_2, 10% N_2). This experiment used zeolite ZSM-5 in ammonium form (CBV-8014, Amberlyst International), $Fe(NO_3)_3 \cdot 9H_2O$ (Merck), $Co(NO_3)_2 \cdot 6H_2O$ (Merck), NaOH p.a. (Merck), nitric acid (Merck), nitric ammonium p.a. (Merck), hydrogen (PT. Samator Gas Industry, Surabaya, Indonesia), synthesis gas (30% CO, 60% H_2, 10% N_2), glass wool, 2 mm glass beads (Marienfeld), and aquadest. One gram of catalyst was utilized in the Fischer-

Tropsch process. The catalyst was combined with glass beads in a ratio of up to six times the weight of the catalyst. The amalgamation of catalyst and glass beads was placed into the catalyst bowl, secured by glass wool at both the bottom and top to avert spillage during the process [18,21]. All catalysts were reduced in situ within the reactor using H_2 gas at a flow rate of 25 mL/min, 1 bar, and 400°C for a duration of 10 hours. Upon completion of the reduction procedure, the reactor was cooled to 250°C, the hydrogen gas flow was terminated, and subsequently, it was substituted with the synthesis gas flow. Certain hydrocarbon fractions were condensed by a heat trap at 30-40°C and 20 bar. The hydrocarbon fraction with a low boiling point would be condensed in a cold trap at 1-10°C and 1 bar. The reaction was conducted for 96 hours, with gas samples collected every 24 hours and liquid samples obtained at the conclusion of the reaction. Gas samples were extracted with a 10 mL syringe and introduced into a 10 mL vacuum bottle (vacutainer).

Gas Chromatography Mass Spectrum (GCMS) was used to measure hydrocarbon composition in the liquid product (GC-MS; HP-Agilent 6890 FID System; Capillary Column: Agilent 19091S-433 HP-5MS; at BRIN, Tangerang, Indonesia). Gas Chromatography with Thermal Conductivity Detector was used to measure the releasing gas (GC 550 P Gas Chromatograph. This device was equipped with a Thermal Conductivity Detector (TCD), Argon as the carrier gas, and a packed column with Molecular Sieve 5A at Instrumental Analysis Laboratory, Department of Chemical Engineering, Universitas Gadjah Mada)

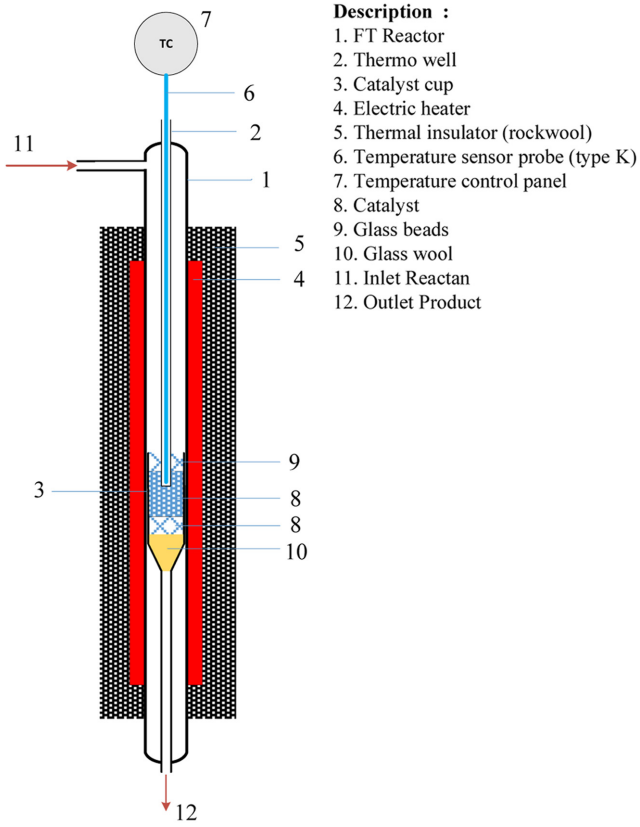

Fig. 1. The schematic of a continuous fixed bed reactor for Fischer-Tropsch synthesis with CO and H_2 synthesis gas feedstock using Fe-Co/meso-HZSM-5 catalyst.

3. Result and Discussion

3-1. Design of continuous fixed bed tubular reactor

The reactor design was adjusted as per the needs of operating conditions including temperature, pressure and gas flow rate. The reactor was designed in such a way that all of these conditions can be maintained stable during the whole process. The addition of control equipment was the key to maintaining these conditions. The tube reactor was designed up to 3 grams catalyst capacity. This design approach emphasized operational stability and simplicity for laboratory-scale applications, while ensuring that critical parameters such as temperature, pressure, and flow rate could be effectively controlled. Detailed design and specifications of reactor parts consisted of dimensions, solid catalyst placement models, controller equipment (flow rate, temperature and gas pressure), hot traps and cold traps for biofuel products on a laboratory scale. The Fischer-Tropsch reactor used (Fig. 1) was made of SS316 stainless steel material with a wall thickness of 2 mm, ID 8 mm, length 80 mm. The relatively small reactor diameter contributed to improved heat and mass transfer characteristics and supported more uniform flow distribution within the packed bed.

Figure 1 showed that the synthetic gas reactant entered horizontally from the upper side of the reactor (11) and exit from the bottom of the reactor (12). The horizontal inlet configuration was selected primarily due to mechanical and fabrication constraints of the laboratory-scale system. The reactor was equipped with a thermo well (2) which was a hole for inserting a sensor rod (6) so that the tip of the sensor remained close to the Fe-Co/meso-HZSM-5 catalyst used during the reaction. Catalyst temperature was a reference in controlling the reaction temperature. The catalyst was placed in a catalyst bowl (3) which was inserted from below the reactor to facilitate catalyst replacement. Glass wool was placed at the bottom of the catalyst bowl to prevent the catalyst powder from being carried by the reactor gas out of the reactor. The catalyst was mixed with glass beads (9) as much as 6 times the weight of the catalyst, adjusting to the volume of the catalyst bowl. The addition of glass beads played an important role in improving flow distribution, reducing channelling, and minimizing pressure drop across the packed bed. Glass beads also helped to reduce the hotspot formation within the catalyst bed during the reaction. Furthermore, the relatively small reactor diameter (8 mm) and low gas flow rate contributed to maintaining a more uniform gas–solid contact, thereby mitigating potential non-ideal flow behaviour associated with horizontal inlet configurations. The design enabled the development of a continuous fixed-bed reactor system using CO and H_2 synthesis gas with Fe–Co/HZSM-5 catalyst, characterized by low pressure drop, controlled gas flow at low flow rates (laboratory scale), and stable temperature and pressure conditions. This configuration

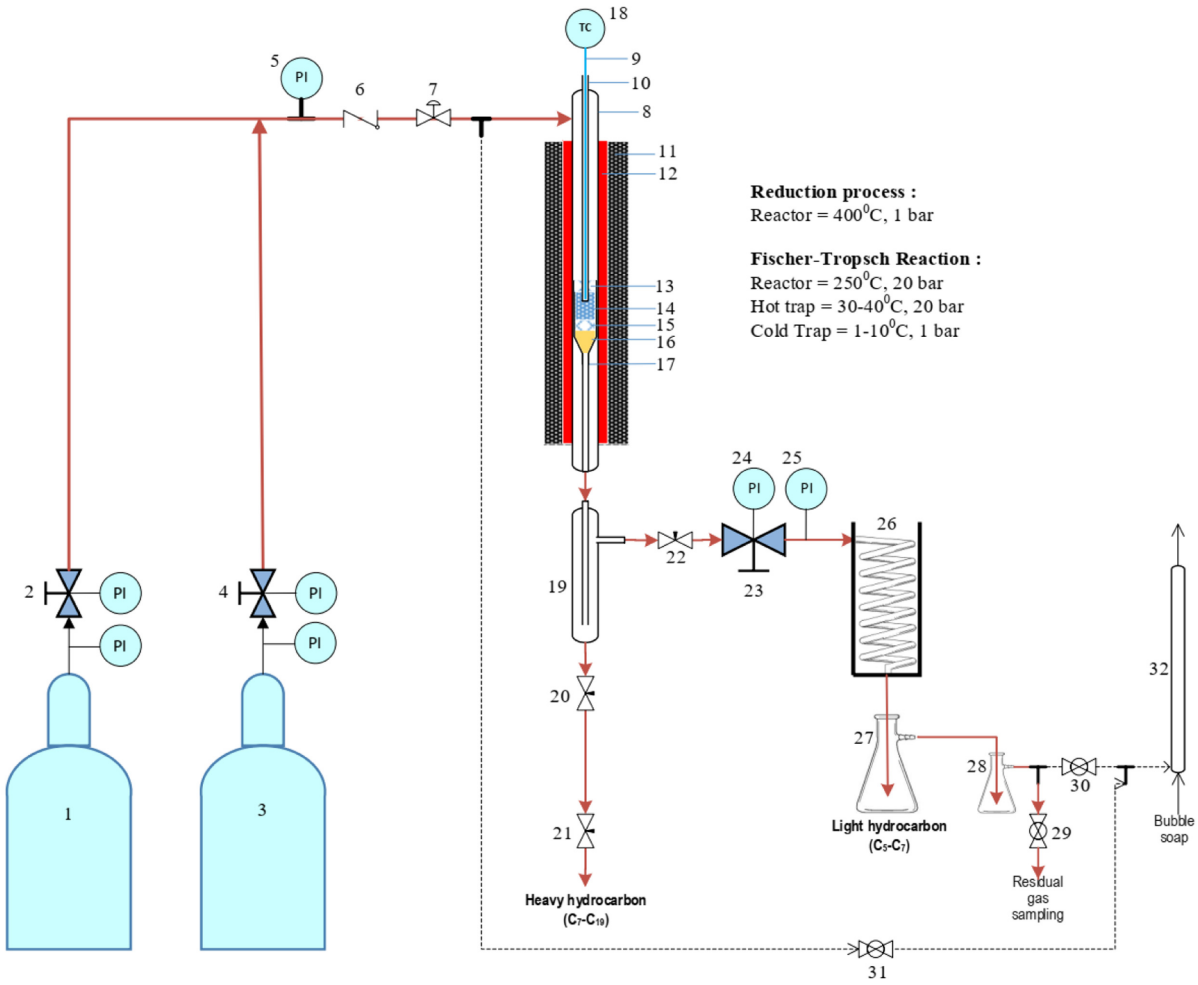

Caption :

1. Hydrogen gas (H_2)
2. Pressure regulator for H_2
3. Synthesis gas (30% CO, 60% H_2, 10% N_2)
4. Pressure regulator for synthesis gas
5. Pressure gauge
6. Check valve
7. Micro metering valve
8. Fischer-Tropsch reactor
9. Temperature probe sensor (type K)
10. Thermo well
11. Heat Isolator (rockwool)
12. Electric Heater
13. Glass beads
14. 10Fe-90Co/mesoHZSM-5 catalyst
15. Glass beads
16. Glass wool
17. Catalyst bowl
18. Temperature panel controller
19. Hot trap
20. Needle valve I (Swagelok)
21. Needle valve II (Swagelok)
22. Ball valve I (Swagelok)
23. Pressure Regulator (modified)
24. Pressure gauge for reactor outlet
25. Pressure gauge for condenser
26. Condenser (cold trap)
27. Separator for liquid and gas product
28. Bubble gas indicator
29. Ball valve II (Sankyo)
30. Ball valve III (Sankyo)
31. Needle valve III (Swagelok)
32. Bubble soap meter

Fig. 2. The schematic of a complete equipment for Fischer-Tropsch synthesis with CO and H_2 synthesis gas feedstock using Fe-Co/meso-HZSM-5 catalyst.

supported reliable operation under laboratory conditions while maintaining simplicity and ease of maintenance. Low and medium boiling point hydrocarbon products can be separated using simple hot trap and cold trap system.

The Flow Back Pressure Regulator (BPR) is commonly used to control reactor pressure in several previous studies. Some BPR brands, such as Swagelok® or Equilibar®, are priced at USD 20,000–35,000 per unit, which poses a challenge for research with limited funding. A double-stage gas regulator can serve as an alternative to BPR, offering equivalent performance at a significantly lower cost. Brands like Harris®, Victor®, and Yamato® provide regulators priced at USD 220–400 for a maximum operating pressure of 30 bar. In this study, a double-stage regulator

Fig. 3. The modified pressure regulator to control the pressure in the reactor and the pressure out of the reactor.

was selected to improve pressure stability and minimize fluctuations compared to single-stage regulators. The regulator was configured at the reactor outlet to provide a constant flow restriction, enabling effective control of upstream reactor pressure under laboratory-scale conditions. Modifications involved replacing the input and output connectors with fitting connectors compatible with the reactor system's piping dimensions. The input connector was connected to the reactor to maintain a pressure of 20 bar, while the output connector was directly vented to the atmosphere at 1 bar. Pressure gauges were installed both upstream and downstream of the regulator to monitor system performance and ensure stable pressure control throughout the operation. The pressure profile during the initial operation period is shown in Fig. 4. Experimental observations showed that the pressure fluctuated slightly during the initial stage (first 14 minutes) within 20 bar ± 0.2 bar and remained stable thereafter during continuous operation. This indicated that the modified regulator provided sufficient pressure control for laboratory-scale applications, although it did not fully replicate the internal mechanism of a commercial back-pressure regulator. To minimize the risk of clogging and pressure instability due to condensable products, the reactor system was equipped with hot and cold traps upstream of the regulator to remove heavy hydrocarbons and condensable compounds before entering the pressure control unit.

The reaction temperature of 250°C was attained at the 11th minute, at which point the heater was automatically turned off. The heat flow entering the system caused the temperature to rise further to 261°C, then decreased back to 250°C, at which point the heater was turned on again. The temperature continued to drop to 243°C before rising again, fluctuating until reaching a steady state starting at the 15th minute, within the range of 250°C ± 3°C. At a reaction temperature setting of 275°C, this condition reached at the 13th minute and achieved a steady state starting at the 18th minute within the range of 275°C ± 4°C. The observed temperature overshoot and subsequent fluctuations were primarily caused by the thermal inertia of the system and the response delay of the contactor-based on–off control mechanism. When the heater was switched off at the setpoint temperature, residual heat stored in the reactor body, insulation, and heating element continued to be released, resulting in a temporary increase in temperature above the setpoint. In addition, the non-instantaneous response of the control system led to a delay between temperature detection and heater switching, further contributing to temperature oscillations. Heat loss to the surrounding environment also influenced the cooling phase, causing the temperature to drop below the setpoint before rising again. Despite these fluctuations, the system reached a stable operating condition within a relatively short time, indicating that the temperature control system performed adequately for laboratory-scale operation. Considering the small reactor dimensions and limited heat generation, the risk of thermal runaway was minimal under the studied conditions.

Statistical analysis was conducted for pressure and temperature

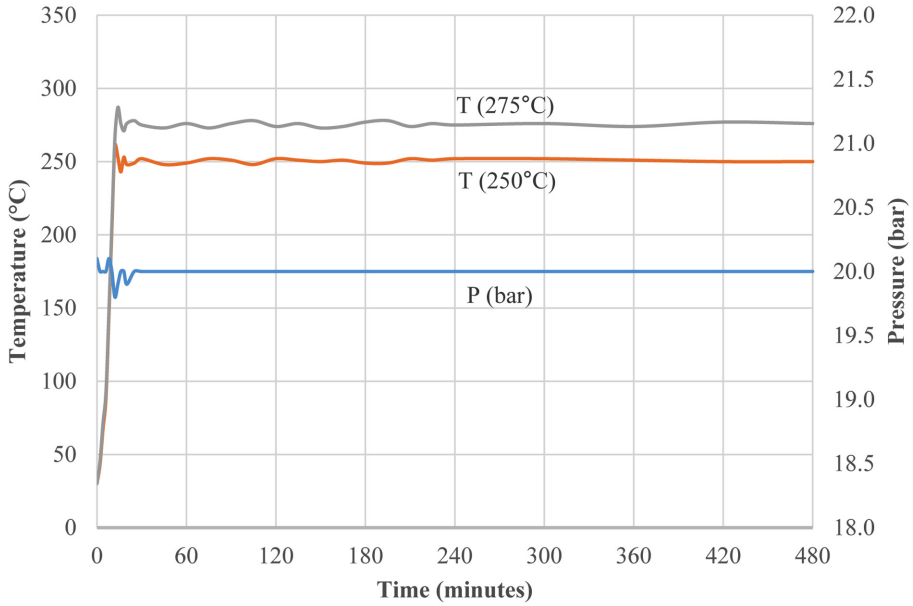

Fig. 4. Temperature and pressure profile in the first 8 hours of Fischer-Tropsch Synthesis at 250°C and 275°C, 20 bar.

(250°C and 275°C) after the 11th minute (reached condition). After the 11th minute, the data indicated that the system pressure remained relatively stable, with an average of 19.98 bar, a standard deviation of 0.07 bar, and minimum and maximum values of 19.8 bar and 20.1 bar, respectively. The 95% confidence interval for pressure was 19.96 bar to 20.00 bar, indicating stable pressure throughout the process. For the 250°C temperature, the recorded average temperature was 250.73°C, with a standard deviation of 3.18°C. The maximum and minimum temperatures observed were 261°C and 243°C, respectively, with a 95% confidence interval of 249.32°C to 252.14°C. This suggested that the heating system maintained the temperature close to the target with minor fluctuations. Meanwhile, for the 275°C temperature, the recorded average temperature was 275.40°C, with a standard deviation of 3.51°C. The maximum observed temperature was 287°C, while the minimum was 266°C. The 95% confidence interval for this temperature was 273.95°C to 276.85°C, indicating relatively stable temperature control despite slight variations. The observed temperature fluctuations were consistent with the dynamic response of the on–off control system and the thermal inertia of the reactor, where residual heat continue to be released after the heater was switched off, leading to temporary overshoot. In addition, heat loss to the surroundings contributed to temperature oscillations around the setpoint. Overall, the system successfully maintained stable pressure and temperature after the 11th minute, despite minor temperature fluctuations. This suggested that the control system was functioning effectively to regulate operational parameters. Considering the laboratory-scale reactor dimensions and low catalyst loading, the heat generated from the reaction was relatively limited, thereby reducing the risk of thermal runaway. Further optimization, such as adjusting the heater control or improving thermal insulation, may help to minimize temperature fluctuations and enhance system efficiency.

The heating system consisted of a heater, thermocouple, temperature controller, contactor, and relay (Fig. 5). The selection of the heater was influenced by the planned operating temperature. A ceramic heater was more suitable for operating temperatures of 200-500°C. The ceramic heater used was customized to evenly cover the reactor body. A power rating of 1500 Watts was utilized to achieve the operating temperature relatively faster. The heater was equipped with a heat insulator made of 2 cm thick rockwool, capable of withstanding temperatures up to 600°C. However, heat loss to the surrounding environment remained significant, indicating that additional insulation thickness may further improve thermal efficiency and temperature stability. A Type K thermocouple probe, 30 cm in length (operating temperature range: -50 to 1200°C), was selected to support the temperature control system. The RKC REX-C100 temperature controller was a digital temperature control device used to regulate and maintain the temperature in a system according to a predetermined setpoint. Its main function was to measure and control reactor temperature by adjusting power supplied to the heating element. The system employed a combination of a relay and a contactor to control electrical flow to the heater. The thermocouple measured the reactor temperature and sent signals to the controller. When the temperature reached the setpoint, the controller triggerd the relay to deactivate the contactor, thereby switching off the heater. The observed temperature fluctuations were primarily caused by the on–off control mechanism and the response delay of the contactor system. When the heater was switched off at the setpoint temperature, residual heat stored in the heating element and reactor body continued to be released due to thermal inertia, resulting in a temporary temperature overshoot.

This behavior was also influenced by heat loss and the dynamic response of the control system, leading to fluctuations within ±3–4°C around the setpoint. Despite these variations, the system maintained a relatively stable temperature range, which was considered acceptable for laboratory-scale operation. In addition, the relatively small reactor dimensions (ID 8 mm) and low catalyst loading limited the heat generated from the Fischer–Tropsch reaction, thereby reducing the risk of thermal runaway. For applications requiring higher temperature precision or scale-up conditions, more advanced control strategies such as improved insulation, PID tuning, or proportional control systems may be required.

3-2. Reactor performance test

The Fischer–Tropsch synthesis (FTS) reaction produced two liquid phases, each exhibiting a distinct pungent odor. The liquid products

(a) (b) (c)

Fig. 5. The homemade ceramic heater (a), thermocouple probe (b), and temperature control RKC REX C100 (c) (https://www.rkcinst.co.jp/english/products/4041/) to maintain the operating temperature.

were collected from the hot trap chamber (30–40°C). Both phases showed similar viscosity, where the upper layer appeared clear yellow, while the lower layer was colorless. Based on GC-MS analysis, the upper layer predominantly consisted of hydrocarbons, mainly alkanes (paraffins), with minor amounts of alkenes (olefins). The lower layer was likely dominated by an aqueous phase (reaction water), containing dissolved oxygenated compounds such as carboxylic acids, alcohols, esters, and aromatic compounds. The product distribution in the upper layer was influenced by catalyst weight. With 1 g of catalyst, the alkane fraction reached 85.04%, while alkenes accounted for 7.56%. Increasing the catalyst weight to 1.2 g raised the alkane fraction to 96.33%, and further increase to 1.4–1.6 g resulted in an alkane fraction of up to 99.96%. Straight-chain hydrocarbon selectivity was also relatively high (57–72%), with the highest value (72.03%) obtained at 1.6 g catalyst. This trend can be explained not only by the increase in catalyst amount but also by the decrease in gas hourly space velocity (GHSV), which led to longer residence time within the reactor. The extended residence time promoted secondary reactions such as olefin hydrogenation and chain growth, resulting in higher alkane selectivity and increased formation of straight-chain hydrocarbons. The reactant composition, with an H_2/CO ratio of 2, also favored hydrogenation reactions. Under these conditions, intermediate olefins were likely further converted into paraffins before exiting the reactor, contributing to the high alkane selectivity. It should be noted that the product distribution was based on GC-MS peak area analysis, which provided semi-quantitative information. Therefore, the reported values represented relative compositions rather than absolute yield.

The combination of polymerization using metal catalyst (Fe-Co) and cracking (meso-HZSM-5) in the FTS intended to produce saturated C_5-C_{19} hydrocarbons (gasoline, kerosene and diesel oil). The desilicated HZSM-5 exhibited mesoporous properties with a diameter ranging from 6.1 to 29.9 nm, an average mesoporous volume of 0.3496 cc/g, and a pore surface area of 526.04 cc/g, as determined by BET analysis. EDX analysis revealed a Si/Al ratio of 22.11 and a metal loading of 16.11% by weight on meso-HZSM-5. The reduced catalyst displayed characteristic XRD peaks corresponding to Fe (66°), Fe-Co alloy (44.50°), and Co_3O_4 (36.80°), indicating successful incorporation of active metal phases.

The product distribution based on hydrocarbon chain length for both liquid layers is presented in Fig. 6 and Fig. 7. The upper layer was dominated by alkane hydrocarbons in the range of C_7–C_{25}. At lower catalyst weights (1.0–1.2 g), the product distribution was mainly concentrated in the C7–C19 range, while only trace amounts of heavier hydrocarbons (C20–C25) were detected. As the catalyst weight increased, the presence of heavier hydrocarbons became more noticeable, although their fraction remained relatively low (<1.7%). This trend was more appropriately explained by changes in gas hourly space velocity (GHSV) rather than catalyst amount alone. Increasing catalyst weight at a constant flow rate reduced GHSV and increased residence time, allowing intermediate species to undergo further chain growth and hydrogenation reactions, leading to the formation of heavier hydrocarbons. The Fischer–Tropsch reaction using 10Fe–90Co/meso-HZSM-5 catalyst at 250°C produced gasoline, kerosene, and diesel fractions. Kerosene was the dominant fraction (55.18–61.68%) across all catalyst weights. The gasoline fraction (C_5–C_9) was highest at 1 g catalyst (19.15%) and decreased with increasing catalyst weight, while the diesel fraction (C_{15}–C_{19}) increased with catalyst loading,

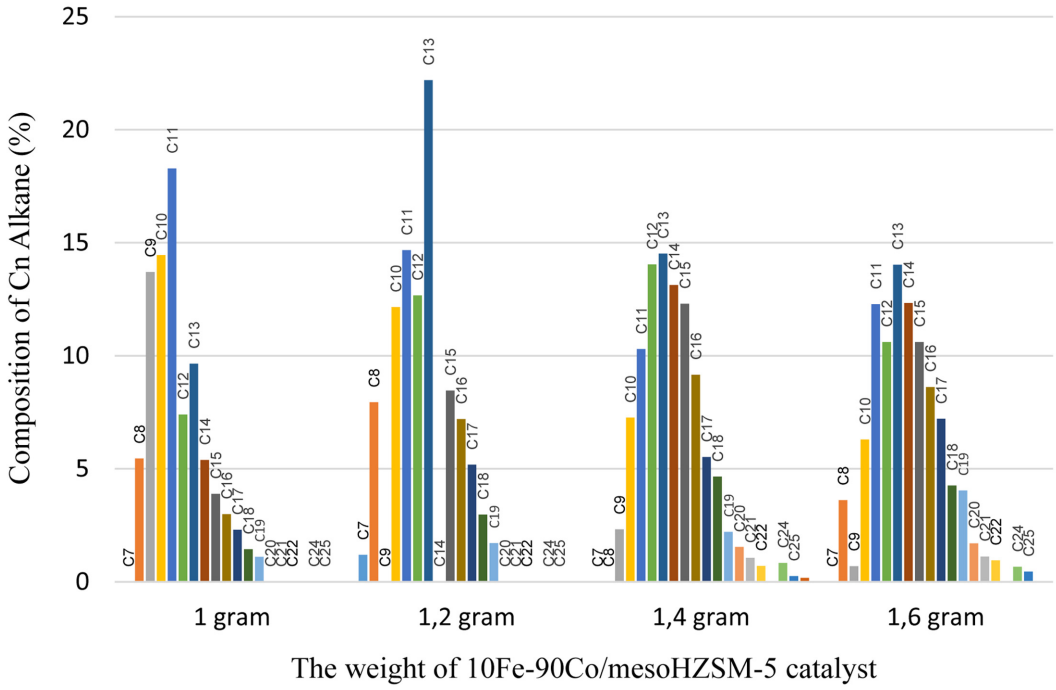

Fig. 6. Distribution of upper layer liquid products from Fischer-Tropsch reaction with catalyst 10Fe-90Co/meso-HZSM-5, loading 10%, synthesis gas (30% CO, 60% H_2, 10% N_2), 25 mL/min, 250°C, 20 bar , 96 hours at various catalyst weight variation (1; 1.2; 1.4; 1.6 gram).

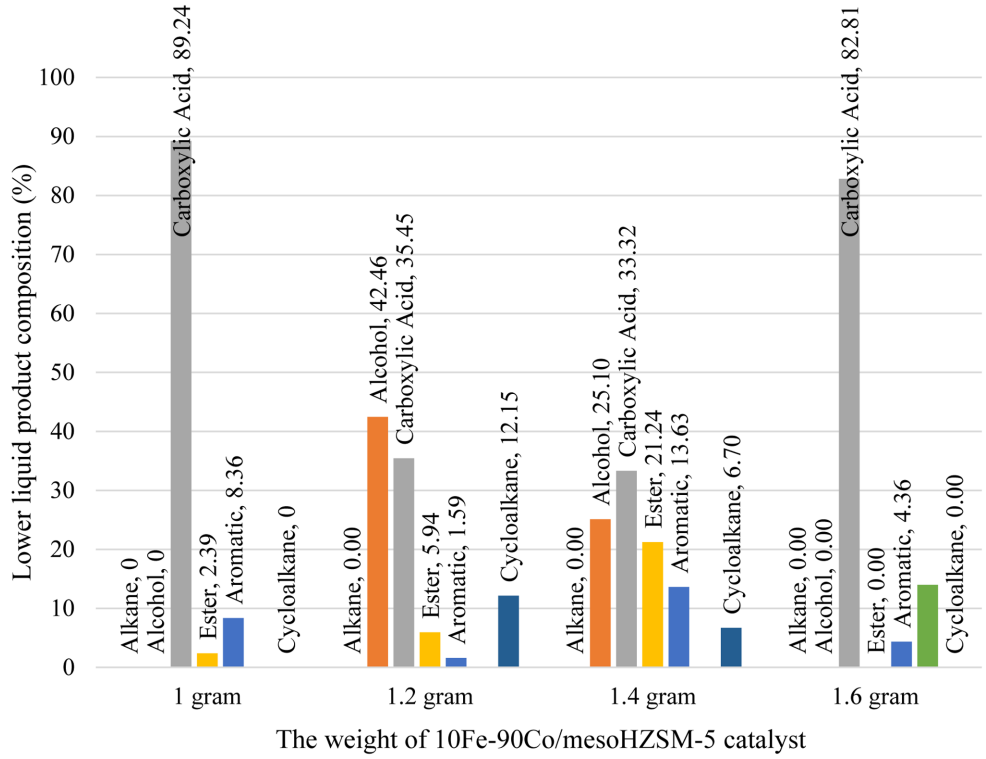

Fig. 7. Distribution of lower layer liquid products from Fischer-Tropsch reaction with catalyst 10Fe-90Co/meso-HZSM-5, loading 10%, synthesis gas (30% CO, 60% H_2, 10% N_2), 25 mL/min, 250°C, 20 bar , 96 hours at various catalyst weight (1; 1.2; 1.4; 1.6 gram).

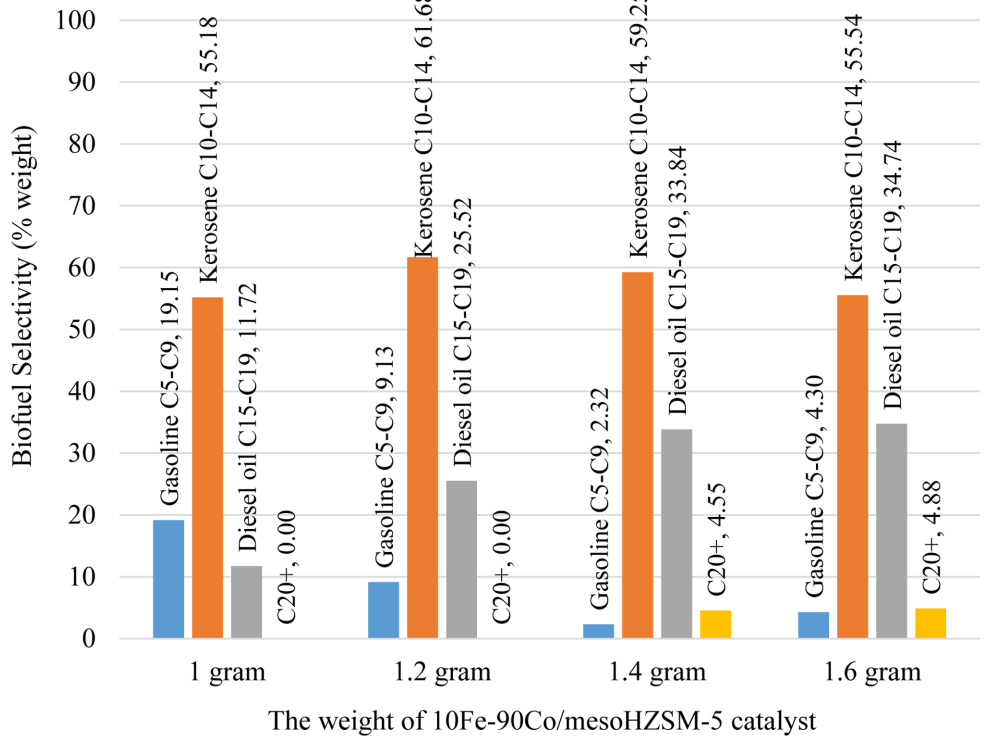

Fig. 8. The selectivity of biofuel (gasoline, kerosene and diesel fuel) to the 10Fe-90Co/meso-HZSM-5 catalyst weight in the 250°C, 20 bar Fischer-Tropsch reaction of using synthesis gas (30% CO, 60% H2, 10% N2) for 96 hours.

reaching 19.34% at 1.6 g.

This shift in product distribution from lighter to heavier hydrocarbons was consistent with increased residence time, which enhanced secondary reactions such as chain propagation and olefin hydrogenation. As a result, longer hydrocarbon chains were formed, leading to a higher diesel fraction and a corresponding decrease in gasoline fraction. It

should be noted that these values represented relative product distribution based on GC-MS peak area analysis, and therefore should not be interpreted as absolute yield or conversion.

The Fischer–Tropsch synthesis (FTS) reaction in this study produced two distinct liquid product layers, with alkane-rich hydrocarbons dominating the upper layer and oxygenated compounds such as carboxylic acids, alcohols, and esters present in the lower layer. The hydrocarbon product distribution was influenced by catalyst loading, with a higher catalyst weight (1.6 g) resulting in increased alkane selectivity (up to 99.96%) and straight-chain hydrocarbon selectivity of 72.03%. However, this trend should be interpreted in relation to gas hourly space velocity (GHSV). Increasing catalyst weight at a constant gas flow rate effectively reduced GHSV and increased residence time, which enhanced secondary reactions such as olefin hydrogenation and chain growth. As a result, longer-chain hydrocarbons are formed, leading to higher alkane selectivity and increased straight-chain hydrocarbon fractions. The product selectivity varied depending on the hydrocarbon chain length, where C_7-C_{19} fractions were predominant when using 1-1.2 g catalyst, while C_{20}-C_{25} hydrocarbons were minimally produced (<1.7%) and became more detectable as catalyst weight increased.

Several studies have examined the product distribution in Fischer-Tropsch synthesis employing various catalyst compositions and reaction settings. Pandey *et al*. [7] indicated that cobalt-based catalysts predominantly yield longer-chain hydrocarbons (wax and diesel-range fuels), while iron-based catalysts preferentially generated gasoline and olefins. This corresponds with our research, wherein the Fe-Co/meso-HZSM-5 catalyst yielded substantial proportions of kerosene (55.18-61.68%) and diesel fuel (up to 19.34%) at 250°C and 20 bar. Gasoline selectivity (C_5-C_9) diminished with increasing catalyst weight, matching the findings of Teimouri *et al*. [8], who observed that elevated catalyst loadings resulted in longer hydrocarbon chains due to intensified hydrogenation processes. Furthermore, Sineva et al. [22] demonstrated that HZSM-5 zeolite can facilitate the cracking of long-chain hydrocarbons, thereby influencing product distribution toward gasoline and kerosene fractions. In this study, the meso-HZSM-5 component likely contributed to hydrocracking activity, maintaining a balance between middle distillates and lighter hydrocarbons. In contrast to Mirzaei *et al.* [23], who reported higher gasoline yields using Fe–Co–Ni catalysts, the Fe–Co catalyst system used in this work showed a higher diesel fraction, which may be attributed to differences in metal composition, active site distribution, and reaction conditions.

It should be noted that the reported product distribution was based on GC-MS peak area analysis, which provided semi-quantitative information. Therefore, these values represented relative composition rather than absolute yield or conversion.

In order to ensure consistent temperature and reactant distribution during scale-up of the Fischer–Tropsch reactor, heat and mass transfer considerations became increasingly important. Stable pressure and flow control will require more advanced regulation systems. Catalyst performance is also critical, as challenges such as sintering and deactivation may require improved bed design and regeneration strategies. Product separation systems may need further optimization to handle higher production volumes. Future work will focus on pilot-scale validation to evaluate the reactor performance under more realistic operating conditions, ensuring efficient, stable, and economically viable biofuel production.

4. Conclusion

This study presented the design and evaluation of a continuous fixed-bed tubular reactor for Fischer–Tropsch synthesis (FTS) under laboratory-scale conditions. The reactor demonstrated stable operation, with pressure maintained at 20 bar (±0.2 bar) and temperature fluctuations within ±3–4°C after reaching steady-state conditions. The integration of a double-stage regulator as a cost-effective alternative to a conventional back-pressure regulator (BPR), along with temperature control and product trapping systems, enabled reliable and continuous reactor performance.

Product analysis based on GC-MS indicated that the liquid products consisted of two distinct phases, with hydrocarbon-rich fractions dominating the upper layer and oxygenated compounds present in the lower layer. The hydrocarbon distribution was primarily composed of alkanes (C7–C25), with kerosene-range hydrocarbons as the dominant fraction. The increase in alkane selectivity and heavier hydrocarbon fractions with increasing catalyst weight was attributed not only to catalyst loading but also to reduced gas hourly space velocity (GHSV) and increased residence time, which further promoted secondary reactions such as hydrogenation and chain growth.

Overall, the reactor design demonstrated stable and reliable performance for laboratory-scale FTS applications. The results presented were based on GC-MS peak area analysis and therefore represent relative product distribution rather than absolute yield. Future work will focus on improving temperature control precision, enhancing insulation, and scaling up the reactor system to evaluate performance under pilot-scale conditions.

References

1. Borg, Ø., Eri, S., Blekkan, E. A., Storsæter, S., Wigum, H., Rytter, E. and Holmen, A., "Fischer-Tropsch Synthesis over γ-alumina-supported Cobalt Catalysts: Effect of Support Variables. *J. Catal.* **248**, 89-100(2007).
2. Mousavi, S., Zamaniyan, A., Irani, M. and Rashidzadeh, M., "Generalized Kinetic Model for Iron and Cobalt Based Fischer-Tropsch Synthesis Catalysts: Review and Model Evaluation," *Appl Catal. A.* **506**, 57-66(2015).
3. Anderson, R. B., Feldman, J. and Storch, H. H., "Synthesis of Alcohols by Hydrogenation of Carbon Monoxide," *Ind. Eng. Chem.* **44**, 2418-2424(1952).
4. Jimmy, R. A., Suprapto, K. F., "Synthesis and Characterization of Fe-Co/mesoHZSM-5: Effect of Desilication Agent and Iron-cobalt Composition," *Korean Chemical Engineering Research*, **58**, 163-169(2020).

5. Ghaani, M. R., Schicks, J. M. and English, N. J., "A Review of Reactor Designs for Hydrogen Storage in Clathrate Hydrates," *Applied Sciences (Switzerland)* **11**, 1-16(2021).
6. Vera, E. D., Peña, C. A. and Bolívar, L. R., "Mechanical Design for High-pressure Reactor to Microwave-assisted Leaching of Refractory Metals," *ARPN Journal of Engineering and Applied Sciences* **17**, 303-311(2022).
7. Pandey, U., Runningen, A., Gavrilović, L, Jørgensen, E. A., Putta, K. R., Rout, K. R., Rytter, E., Blekkan, E. A., Hillestad, M., "Modeling Fischer–Tropsch Kinetics and Product Distribution over a Cobalt Catalyst," *AIChE Journal* **67**, 1-15(2021).
8. Teimouri, Z., Abatzoglou, N. and Dalai, A. K., "Kinetics and Selectivity Study of Fischer-tropsch Synthesis to c^{5+} Hydrocarbons: A Review," *Catalysts* **11**, 1-32(2021).
9. Sonal, K. K., Pant, K. K. and Upadhyayula, S., "Synergistic Effect of Fetextendashco Bimetallic Catalyst on FTS and WGS Activity in the Fischertextendashtropsch Process: A Kinetic Study," *Ind Eng Chem Res.* **56**, 4659-4671(2017).
10. Balivada, R., Apparatus And Process For Gas To Liquid (Gtl) Conversion. 13(2012).
11. Griboval-Constant, A., Butel, A., Ordomsky, V. V., Chernavskii, P. A. and Khodakov, A. Y., "Cobalt and Iron Species in Alumina Supported Bimetallic Catalysts for Fischer-Tropsch reaction," *Appl Catal A Gen*. **481**, 116-126(2014).
12. Mousavi, S., Zamaniyan, A., Irani, M. and Rashidzadeh, M., "Generalized Kinetic Model for Iron and Cobalt Based Fischer-tropsch Synthesis Catalysts: Review and Model Evaluation," *Appl Catal A Gen.* **506**, 57-66(2015).
13. Mahmoud Aboelkheir, I. M., "An Optimized Chemical and Mechanical Engineering Design of an Ammonia Reactor," *Cognizance Journal of Multidisciplinary Studies* **2**, 10-37(2022).
14. Abdollahi, M., Atashi, H., Tabrizi, F. F. and Mansouri, M., "Fischer–Tropsch Study over Impregnated Silica-supported Cobalt–iron Nanocatalyst," *Journal of the Iranian Chemical Society.* **14**, 245-256(2017).
15. Nakhaei, P. A. and Housaindokht, M. R., "A New Kinetic Model for Direct CO_2 Hydrogenation to Higher Hydrocarbons on a Precipitated Iron Catalyst: Effect of Catalyst Particle Size," *Journal of Energy Chemistry.* **26**, 359-367(2017).
16. Sineva, L. V., Asalieva, E. Y. and Mordkovich, V. Z., "The Role of Zzeolite in The Fischer–Tropsch Synthesis over Cobalt–Zeolite Catalysts," *Russian Chemical Reviews* **84**, 1176-1189(2015).
17. Arsalanfar, M., Mirzaei, A. A., Bozorgzadeh, H. R., Samimi, A. and Ghobadi, R., "Effect of Support and Promoter on the Catalytic Performance and Structural Properties of the Fe-Co-Mn Catalysts for Fischer-Tropsch Synthesis," *Journal of Industrial and Engineering Chemistry* **20**, 1313-1323(2014).
18. Al Fatony, Z., Resha, A. H., Persada, G. P., Makertihartha, I. G. B. N., Gunawan, M. L. and Subagjo, S., "Effects of Cu on the Modified Co-based Catalyst Activity for Fischer-tropsch Synthesis," *ASEAN Journal of Chemical Engineering*. **18**, 60-67(2018).
19. Borg, O., Eri, S., Blekkan, E. A., Storsæter, S., Wigum, H., Rytter, E. and Holmen, A., "Fischer-Tropsch Synthesis over γ-alumina-supported Cobalt Catalysts: Effect of Support Variables," *J. Catal.* **248**, 89-100(2007).
20. Guettel, R., Kunz, U. and Turek, T., "Reactors for Fischer-Tropsch synthesis," *Chem Eng Technol*. **31**, 746-754(2008).
21. Al Fatony, Z., Febriani, Y., Makertihartha, I., Gunawan, M. L. and Subagjo, S., "Acidity Effects of K Promoted Co-based Catalyst with NH_4 OH Addition of the Impregnation Solution for Fischer-Tropsch Synthesis," *MATEC Web of Conferences*. **268**, 1-5(2019).
22. Sineva, L. V., Asalieva, E. Y. and Mordkovich, V. Z., "The Role of Zeolite in The Fischer–Tropsch Synthesis over Cobalt–Zeolite Catalysts," *Russian Chemical Reviews* **84**, 1176-1189(2015).
23. Mirzaei, A. A., Sarani, R., Azizi, H. R., Vahid, S. and Torshizi, H. O., "Kinetics Modeling of Fischer-Tropsch Synthesis on the Unsupported Fe-Co-Ni (ternary) Catalyst Prepared Using co-precipitation Procedure," *Fuel.* **140**(15), 701-710(2015).

Authors

Jimmy: Lecturer, Department of Chemical Engineering, National Institute of Technology (ITN) Malang, Jln. Bendungan Sigura-gura No. 2, Malang, East Java 65145, Indonesia; j_roring@yahoo.com

Endah Kusuma Rastini: Lecturer, Department of Mechanical Engineering, National Institute of Technology (ITN) Malang, Jln. Bendungan Sigura-gura No. 2, Malang, East Java 65145, Indonesia

Aman Santoso: Lecturer, Department of Chemistry, Malang State University, Jln. Semarang No. 5, Malang, East Java 65145, Indonesia

Elvianto Dwi Daryono: Lecturer, Department of Chemical Engineering, National Institute of Technology (ITN) Malang, Jln. Bendungan Sigura-gura No. 2, Malang, East Java 65145, Indonesia